Journal of Rock Mechanics and Geotechnical Engineering 7 (2015) 700–707

Contents lists available at ScienceDirect

Journal of Rock Mechanics and Geotechnical Engineering

journal homepage: www.rockgeotech.org

Full length article

A distributed measurement method for in-situ soil moisture content by using carbon-fiber heated cable

Dingfeng Cao [a], Bin Shi [a,*], Honghu Zhu [a,*], Guangqing Wei [b], Shen-En Chen [c], Junfan Yan [a]

[a] School of Earth Sciences and Engineering, Nanjing University, Nanjing, 210023, China
[b] Suzhou NanZee Sensing Technology Co., Ltd., Suzhou, 215123, China
[c] Department of Civil and Environmental Engineering, University of North Carolina at Charlotte, NC 28223, USA

ARTICLE INFO

Article history:
Received 15 April 2015
Received in revised form
20 August 2015
Accepted 24 August 2015
Available online 3 October 2015

Keywords:
In-situ soil moisture content
Distributed measurement
Carbon-fiber heated cable (CFHC)
Fiber-optic sensing

ABSTRACT

Moisture content is a fundamental physical index that quantifies soil property and is closely associated with the hydrological, ecological and engineering behaviors of soil. To measure in-situ soil moisture contents, a distributed measurement system for in-situ soil moisture content (SM-DTS) is introduced. The system is based on carbon-fiber heated cable (CFHC) technology that has been developed to enhance the measuring accuracy of in-situ soil moisture content. Using CFHC technique, a temperature characteristic value (T_t) can be defined from temperature–time curves. A relationship among T_t, soil thermal impedance coefficient and soil moisture content is then established in laboratory. The feasibility of the SM-DTS technology to provide distributed measurements of in-situ soil moisture content is verified through field tests. The research reported herein indicates that the proposed SM-DTS is capable of measuring in-situ soil moisture content over long distances and large areas.

1. Introduction

Soil moisture content is an important and fundamental physical index that correlates to the hydrological, ecological and engineering properties of soil (Maleki and Bayat, 2012; Mittelbach et al., 2012; Cho and Choi, 2014). To obtain accurate and reliable in-situ soil moisture content is imperative for solving many engineering problems. In laboratory, the most direct and common method for measuring soil moisture content is the drying method. Obviously, this method is not directly applicable to field conditions, where the capability of measuring over large areas and long distances is an essential requirement (Schmugge et al., 1980; Lunt et al., 2005; Yin et al., 2013).

There are also several in-situ methods for measuring soil moisture content that have been suggested, including the time domain reflectometry (TDR) method, the capacitance and frequency domain reflectometry (FDR) method, the ground penetrating radar (GPR) method, and remote sensing methods (Dobriyal et al., 2012). Each proposed method has its own advantages, disadvantages and limiting scope. All the above-mentioned methods, however, do share a common weakness, that they provide only point-mode measurements and cannot satisfy the real-time measuring requirement of in-situ soil moisture content (Dobriyal et al., 2012; Susha Lekshmi et al., 2014; Sun et al., 2015). Although GPR and remote sensing methods can obtain soil moisture content distribution on ground surface over an area, their measuring accuracy is poor due to environmental factors, such as vegetation, soil surface temperature, surface reflectivity, and thus the measuring depth is limited to the soil surface (Doolittle and Collins, 1995; Weihermüller et al., 2007; Schrott and Sass, 2008).

Distributed fiber-optic sensing (DFOS) technology for condition monitoring of engineering systems has been rapidly developed in recent years. Compared with other sensing technologies, DFOS technology is superior in that it is capable of distributed and long-distance measurements, characterized by anti-corrosion and anti-jamming. One of the DFOS technologies is the Raman optical time domain reflectometry (ROTDR) technique which has extensive applications to integrity monitoring of electric power structures, tunnels and oil wells. ROTDR has also been applied as fire warning systems and for seepage monitoring in dams. For example, Côté et al. (2007) used optical fibers to detect water leakage at the Peribonka dam, and Vogt et al. (2010) estimated the seepage rates in a losing stream by means of a fiber-optic, high-resolution vertical temperature profiling technique. In application

* Corresponding authors. Tel.: +86 25 85386640.
E-mail addresses: shibin@nju.edu.cn (B. Shi), zhh@nju.edu.cn (H. Zhu).

Peer review under responsibility of Institute of Rock and Soil Mechanics, Chinese Academy of Sciences.
1674-7755
http://dx.doi.org/10.1016/j.jrmge.2015.08.003

of moisture monitoring, some distributed technology and equipment were proposed. These technologies include two types: passive fiber optics (PFO) method and actively heated fiber optics (AHFO) method. For the PFO, there is no external power to heat cable, and soil moisture content is determined by sensing the natural temperature of soil. While for AHFO, an external power is needed to heat cable and produce thermal pulses on soil, and the moisture content is inferred by the spreading characteristics of these thermal pulses.

Because the PFO does not need the heat source, it is an energy-saving and intrinsic-safe method. Steele-Dunne et al. (2010) demonstrated the feasibility of using buried fiber-optic cables as a distributed measurement technique to determine the thermal response of soil moisture to diurnal temperature cycles. Although the PFO is a low-cost method, its precision can be affected by a large number of factors, e.g. temperature difference, plants cover, weather and seasons.

By using an actively heated fiber-optic cable, Weiss (2003) demonstrated the potential for collecting distributed soil moisture content data but with errors >6%. A laboratory test conducted by Sayde et al. (2010) showed that it is possible to use ROTDR system for measurements of active soil moisture content with high precision and short measurement time. They fitted an exponential relation between soil moisture and cumulative temperature increase. Striegl and Loheide (2012) used the similar AHFO method in the field to measure soil moisture content. Ciocca et al. (2012) systematically introduced the basic principles of the AHFO method in heating and cooling phases. Gil-Rodríguez et al. (2012) used the AHFO method to estimate wetting bulbs and water distribution under drip emitters in the laboratory. Benítez-Buelga et al. (2014) obtained volumetric heat capacity and water content by using dual-probe approach. Read et al. (2014) quantified vertical flow in boreholes by the AHFO technology. Sayde et al. (2014) firstly used the AHFO method in a field across 1–1000 m scales.

Although these previous experimental results have demonstrated the feasibility of applying optical fibers for distributed measurement of soil moisture content, further studies are needed to improve the technique including possibly integrating laboratory and field measurements into more efficient methods or developing hybrid cable configurations to optimize heating schemes, etc. (Sayde et al., 2010; Striegl and Loheide, 2012). This is because the thermal property of hybrid cable directly influences the measurement accuracy of soil moisture content, and the heating mode or power supply determines the measurement distance. A perfect heated cable should have uniformity in its axial direction, i.e. the electric resistance should be identical for each section with the same length. Furthermore, the calibration procedure proposed by Sayde et al. (2010) is very complicated and the relationship between soil thermal conductivity and moisture content has not been established. A large number of functions were used to fit the relation between soil thermal conductivity and moisture content, and the most one appears in a form of exponential function, however, all of these are empirical or semi-empirical equations which cannot be obtained from theoretical analytical solution (Chung and Horton, 1987; Côté and Konrad, 2005; Lu et al., 2007; Jougnot and Revil, 2010).

A distributed measurement system for in-situ soil moisture content (SM-DTS) is introduced in this paper. This work aims at promoting the application of optical fiber sensing to soil moisture content in the field, simplifying the calibration procedure, and obtaining a more maneuverable and effective relation between thermal conductivity and moisture content. The following sections will describe the fundamental principles of SM-DTS, the structure of the carbon-fiber heated cable (CFHC), the definition of the temperature characteristic value (T_t) and the relationship among T_t, soil thermal impedance coefficient and soil moisture.

2. Fundamental principle of SM-DTS

Distributed temperature sensing (DTS) technology based on the ROTDR was first proposed by Hartog (1983) that when a pumped laser pulse with a certain amount of energy is launched into a sensing optical fiber, a collision occurs between fiber molecules and photons, which yields spontaneous Raman scattering. As a result, two light photons with different wavelengths are generated, i.e. Stokes light and anti-Stokes light (Grattan and Sun, 2000). According to the relationship between the anti-Stokes/Stokes intensity ratio and the temperature of the optical fiber, the distributed measurement of temperature along the sensing fiber can be realized (Tyler et al., 2009). The most prominent advantage of the Raman scattering spectrum is that it is only sensitive to temperature and single-end measurement, which is very fitting for geotechnical engineering monitoring where measurements are usually deep in the earth. Modern DTS systems have relatively high temperature measurement accuracies at ±0.1 °C, and are capable of long measuring distances at dozens of kilometers. In this paper, an attempt is made to adopt DTS technology to measure in-situ soil moisture content by using the SM-DTS technology. The underlying principle of the SM-DTS technology is based on the assumption that a straightforward relationship between the temperature characteristic value (T_t) and soil moisture content can be established, which can be used to quantify in-situ soil moisture content using a heated cable buried in the tested soil and a DTS sensing unit.

2.1. The carbon-fiber heated cable

In order to enhance the measurement accuracy of the soil moisture content by a DTS unit, a CFHC is suggested and is developed for field applications. Fig. 1 shows a cross-sectional view of the CFHC with 4 mm in diameter, which consists of a multimode optical fiber, a carbon-fiber and a carbon-fiber jacket. The optical fiber contains its own core, cladding, coating and fiber-optic jacket. The optical fiber is then encased by 24,000 carbon-fibers.

The CFHC is heated by the conduction of the carbon-fibers, and the heating principle is shown in Fig. 2. The carbon-fiber is connected to several close-loop electric circuits consisting of two copper wires that are electrically collocated and connected to the carbon-fibers through annular binding posts. The annular binding post is installed with a distance of *D*. One end of the copper wire is connected with the annular binding post, and the other end is connected to a power supply. The heating power of each section of the carbon-fiber between two adjacent annular binding posts should be identical. It is assumed that the carbon-fiber with the

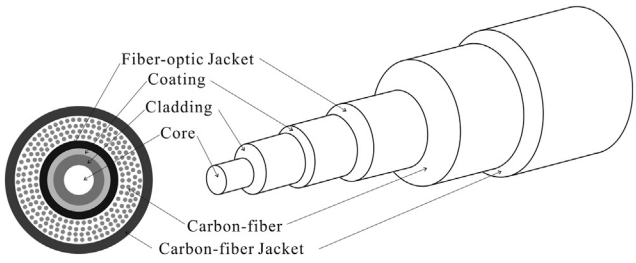

Fig. 1. Cross-sectional view of the CFHC (not to scale).

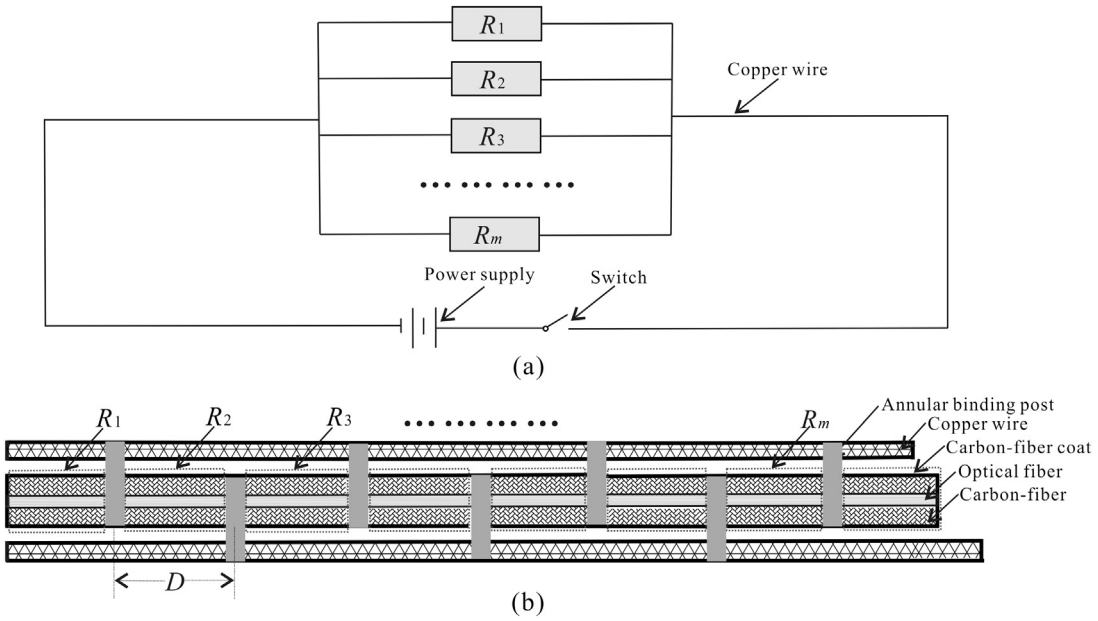

Fig. 2. Diagram for the heating principle of the CFHC. (a) Equivalent circuit diagram of CFHC, and (b) Circuit connection style of CFHC.

same length will have an equivalent resistance of R. The equivalent circuit diagram is shown in Fig. 2a.

In both the laboratory and field tests, the heating power (Q) is set as 2.74 W/m, and the electric current flowing through every equivalent resistance (R) is determined to be 0.378 A. Heat spreading characteristic of the CFHC after conducting heat is shown in Fig. 3 where Q_1 is the energy to heat CFHC itself, and Q_2 is the energy that has been spread into surrounding soil. The sum of Q_1 and Q_2 is the heating power (Q). Since soils with different moisture contents will have disparate thermal impedance coefficients, consequently, the heating temperature–time curves of soils with different moisture contents around the CFCH can also be different.

A typical heating temperature–time curve for soil is shown in Fig. 4. According to the heating rate, the curve can be divided into two stages. The first stage involves temperature rapidly rising within the soil when the conducting carbon-fiber starts to heat up; and the second stage involves the temperature rising rate slowing down (after an initial heating period), eventually becoming plateaued (Côté et al., 2007).

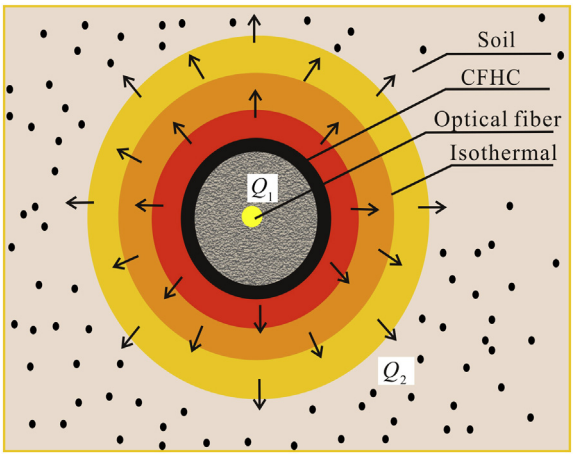

Fig. 3. Diagram for the principle of the soil moisture content measurement technique using SM-DTS.

2.2. Temperature characteristic value

Sayde et al. (2010) have already proposed a temperature variable, cumulative temperature increase, T_{cum}, which is defined as the temperature integration during the total time. They have established an empirical and complicated relation between T_{cum} and soil moisture content. Even though the T_{cum} has many advantages, it is not defined scrupulously, because the temperature is recorded by DTS discretely, and we cannot calculate the integration of these discrete data directly. In order to establish a simple but effective relationship between the temperature distribution along the CFHC, and to overcome the weakness of T_{cum}, a temperature characteristic value (T_t) is proposed, which is defined as the arithmetic mean value of the temperatures measured by the DTS within a defined characteristic time interval of [t_a, t_b]. The temperatures at t_a and t_b are defined as T_a and T_b, respectively in Fig. 4. The time interval is selected based on the temperature–time curve. T_t is calculated as

$$T_t = \frac{\sum_{i=a}^{b} T_i}{n} \quad (1)$$

where T_i is the temperature value measured by DTS within a characteristic time interval [t_a, t_b] and n is the number of measurements during the time interval. On the temperature–time curve, the characteristic time interval is selected based on the tapering stage of the time–temperature curve. T_t is then calculated as shown in Fig. 4.

The factors that affect T_t may come from two aspects. The first one is the intrinsic property of soil itself, such as mineral composition, grain size and dry density; and the second one comes from external elements, such as moisture and environmental temperature (Wierenga et al., 1969; Abu-Hamdeh and Reeder, 2000; Côté and Konrad, 2005; Markle et al., 2006; Abbasy et al., 2014). For a specific in-situ soil, the mineral composition and structural performance typically remain the same. The effect of ambient temperature can be easily compensated by sensor calibration. So the main factor influencing the soil thermal impedance coefficient and T_t is only the soil moisture content. Therefore, once the relationship

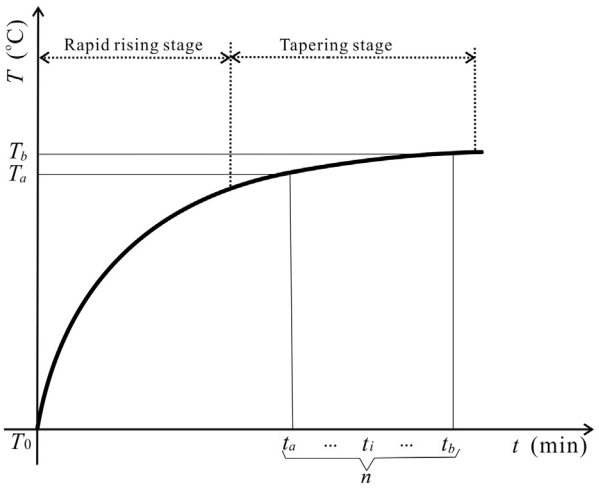

Fig. 4. Temperature–time curve of CFHC during the heating process.

between soil moisture content and T_t is established, the soil moisture content can be easily measured by T_t.

2.3. Relationship between T_t and soil moisture content

Assuming that the soil is uniform and isotropic, for a line thermal source such as CFHC buried in a boundless soil medium, the temperature (T) obtained by DTS satisfies the following relationship (Côté et al., 2007):

$$T - T_0 = \frac{q_L \rho}{4\pi} \ln t + D \tag{2}$$

where q_L is the heat source strength per unit length (W/m); ρ is the thermal impedance coefficient ((m K)/W); T_0 is the initial temperature of the line thermal source; D is a constant for a specific soil, which is independent of time but a function of the medium thermal diffusivity. Eq. (2) can be combined into Eq. (1) and result in:

$$T_t = \frac{q_L \sum_{i=a}^{b} \ln t_i}{4\pi n} \rho + T_0 + D \tag{3}$$

Once the characteristic time interval is selected, $\sum_{i=a}^{b} \ln t_i$ becomes a constant. Then Eq. (3) can be transformed into the following form:

$$T_t = A\rho + B \tag{4}$$

where

$$A = \frac{q_L \sum_{i=a}^{b} \ln t_i}{4\pi n}, \quad B = T_0 + D \tag{5}$$

Both A and B are values to be determined in laboratory or during field tests. The soil thermal impedance coefficient depends on the thermal impedance of solid particles, dry density and moisture content, but for a specific soil, the solid particles and dry density change slightly with time. Therefore, the factor affecting T_t is only the moisture content. According to the results obtained by Sayde et al. (2010), the relation between T_t and moisture content is nonlinear, especially when soil is very dry, but for a large range of soil moisture content, this relation can be approximately regarded as linear:

$$\rho = C\omega + D \ (\omega_1 < \omega < \omega_2) \tag{6}$$

where ω is the soil moisture content, ω_1 is the lower limit of moisture content for the application scope of Eq. (6), and ω_2 is its upper limit. After Eq. (6) is simplified, the relationship between T_t and ω can be written as

$$T_t = E\omega + F \tag{7}$$

where $E = AC$, $F = AD + B$.

According to Eq. (7), it can be obtained that:

$$\omega = kT_t + b \tag{8}$$

where $k = 1/E$ and $b = -F/E$. Both k and b are constants that can be determined through laboratory tests. According to Eq. (8), the soil moisture content can be determined through T_t measurements.

3. SM-DTS design

Based on the description of the SM-DTS principle in previous section, a distributed measurement system for soil moisture content is devised which consists of three subsystems: a heating-sensing unit, a demodulating unit and a data processing unit, as shown in Fig. 5.

The heating-sensing subsystem consists of the carbon-fiber, the sensing optical fiber, the copper wires, the power supply, the annular binding posts and the cable coating, all bundled together. The function of the subsystem is both sensing and transmitting of temperature along the CFHC. The demodulating subsystem includes the DTS demodulation instrument and associated software. Its main function is to transform the light signal in the optical fiber sensor into temperature signal. The data processing subsystem includes both the data processing instrument and associated software, which is used to analyze the data measured by the DTS, to generate the temperature–time curves, and to determine T_t. The soil moisture content can then be calculated from the computed T_t.

As shown in Eq. (8), in the field measuring process, it is not necessary to investigate the basic physical indices such as composition, dry density and grain size as long as the coefficients k and b are calibrated before measurement. When SM-DTS is applied in field for a long time, the temperature sensed by CFHC can be affected by environmental factors, such as climate, season and weather. To avoid this adverse influence, as a rule of thumb, the buried depth of CFHC should be more than 0.2 m.

4. Laboratory test

In order to verify the feasibility of SM-DTS in measuring soil moisture content, calibration tests have been performed in the laboratory.

4.1. Testing scheme

Because the spatial resolution of DTS is only 1 m, so, to improve the spatial resolution, a CFHC with 5 m in length is coiled onto a polyvinyl chloride (PVC) tube of 5 cm in diameter, forming a measuring tube, as shown in Fig. 6.

The spatial resolution of the measuring tube can then be calculated as

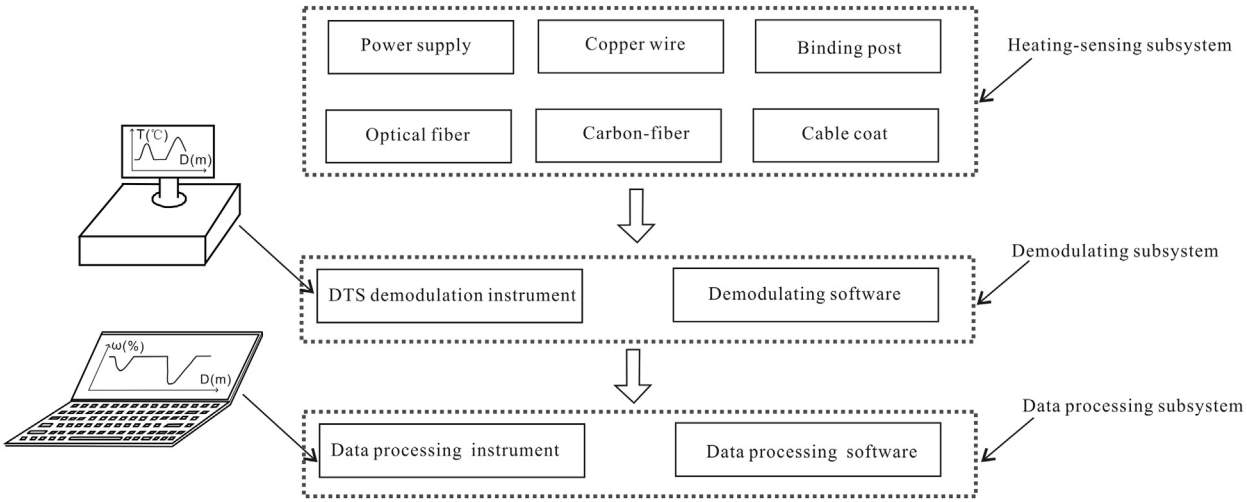

Fig. 5. Schematic diagram of the SM-DTS including heating-sensing subsystem, demodulating subsystem and data processing subsystem.

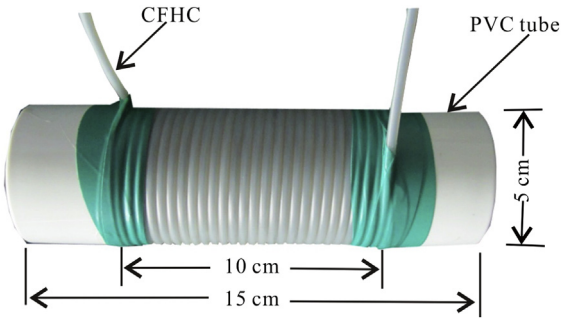

Fig. 6. Forming of the measuring tube.

$$M = \frac{S}{\pi P}\phi \tag{9}$$

where M is the spatial resolution of the measuring tube, ϕ is the diameter of CFHC (4 mm in this study), P is the diameter of the measuring tube (5 cm in this study), and S is the spatial resolution of the DTS (1 m in this case). From Eq. (9), M is computed to be 2.5 cm, showing a significant improvement.

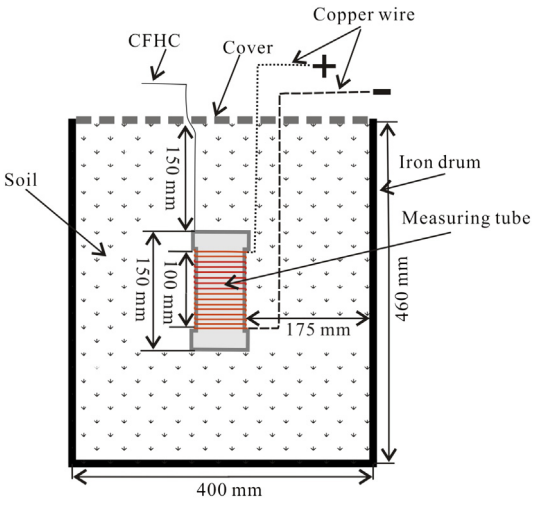

Fig. 7. Basic configuration of laboratory tests.

The laboratory test involved the measurements of clayey soil with different moisture contents. Before measuring, the clayey soil was filled layerwise into an iron drum of 40 cm in diameter and 46 cm in height, and the measuring tube was buried into the center of the iron drum, as shown in Fig. 7. The chemical composition of soil is described in Table 1. The soil was prepared into six groups with moisture contents of 10%, 15%, 25%, 30% and 35%, respectively, and T_t was measured by the SM-DTS.

4.2. Results and discussion

Fig. 8 shows the temperature–time curves for the soil samples with different moisture contents. During moisture content measurement, a nonheating, temperature sensing optical fiber was pasted on the inner wall of the iron drum to measure the boundary temperature within the iron drum. No temperature perturbation on the inner wall was found; hence, the boundary effect of the iron drum can be neglected. The temperature rising time is in the range of 0–23 min, and the temperature will taper at around the time range of 23–30 min. On the temperature tapering stage, the interval of 26–30 min is selected as the characteristic time interval $[t_a, t_b]$ to calculate T_t. The time of the selected interval is 4 min and n is 5.

As can be seen in Fig. 8, the relationship between T and time t appears to be a logarithmic function, which is consistent with the theoretical analysis (Côté et al., 2007). It is found that the deviations between any two neighboring curves are approximately consistent except for that between the 10% and 15% curves. This phenomenon can be established as an optimal proportion of water absorption of 10% moisture content within the soil. When the absorbed water is heated, it did not move freely like free water through molecular movement to spread energy. As a result, the thermal impedance is

Table 1
Chemical composition of the test soil.

Chemical composition	Percentage (%)
SiO_2	56.26
Fe_2O_3	1.04
Al_2O_3	41.92
K_2O	0.66
Na_2O	0.12

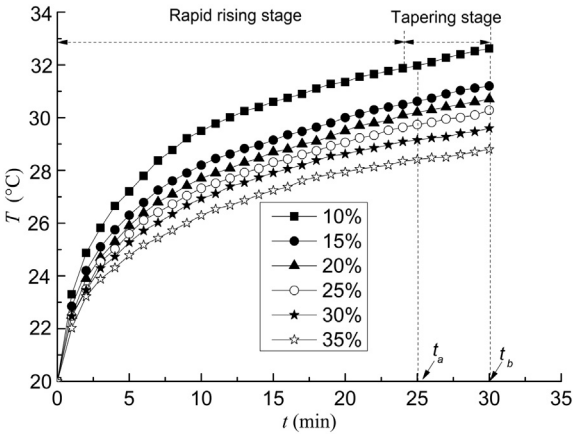

Fig. 8. Temperature–time curves of the measuring tube buried in soils with different moisture contents for 30 min heating under 2.74 W/m power.

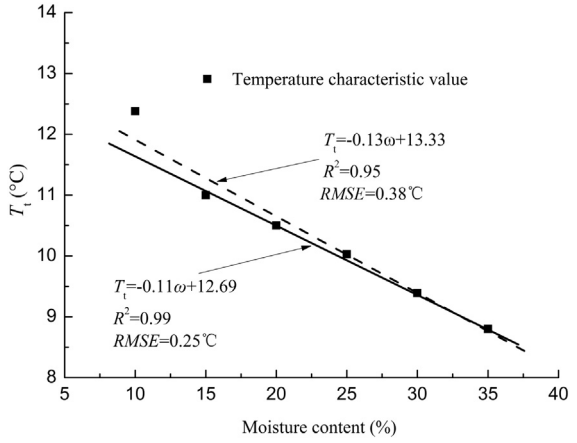

Fig. 9. Relation between T_t and moisture content, ω, with 2.74 W/m heat power. Solid line represents the linear fitting result for soil samples except the sample with 10% moisture content, and the R^2 of fitting function is 0.99. Dashed line represents the linear fitting result for all soil samples, and the R^2 of fitting function is 0.95.

higher, so the corresponding T is higher (Luo and Li, 1990; Barry-Macaulay et al., 2013).

The T_t of the six soil samples during the 30 min heating process are 12.4 °C, 11 °C, 10.5 °C, 10 °C, 9.4 °C and 8.8 °C, respectively. The linear fitting results with moisture content (ω) are shown in Fig. 9.

It can be seen from Fig. 9 that there is a linear relationship between ω and T_t obtained from the soils with moisture contents of 15%, 20%, 25%, 30% and 35%. The coefficient of determination (R^2) is 0.99, and root mean squared error (RMSE) is 0.25 °C, shown as the solid line in Fig. 9. If we consider the T_t obtained from 10% moisture soil into the fitting process, R^2 will decrease to 0.95, and RMSE will increase to 0.38 °C, shown as the dashed line in Fig. 9. Thus, the relationship between ω and T_t can be express as

$$T_t = -0.13\omega + 13.33 \quad (10)$$

Eq. (10) can be expressed as Eq. (11) by some linear transformation steps:

$$\omega = -7.69T_t + 103.53 \quad (11)$$

On the basis of Eq. (11), the soil moisture content can be determined with a determined T_t. Since actual soil composition and dry density have influence on T_t, it is necessary to calibrate the coefficients k and b.

5. Field test

The following field test is conducted to verify the effectiveness of SM-DTS in the field.

5.1. Schematic design of field test

The field test was conducted in a 19 m long trench with silty clay, and its mineral composition is the same as that used in the laboratory tests. The CFHC was buried in the soil directly instead of the measuring tube. Because the field is 19 m in length, 1 m spatial resolution DTS can meet the measurement requests. The heating power in the field was kept the same as that in the laboratory tests. Fig. 10 shows the soil trench with a cross-section of 20 cm × 20 cm. The CFHC was paved at the bottom of the trench, then backfilled and compacted. The trench from A to B was lengthwise divided into three sections where 1–7 m and 13–19 m were with the same moisture content and 7–13 m with less moisture content. After the measurement was made using the SM-DTS, the soil moisture contents of each section were measured using drying method in the laboratory.

5.2. Results and discussion

Comparison of soil moisture content measured by drying method (ω_D) and SM-DTS (ω_S) is shown in Fig. 11. It can be seen from Fig. 11 that the variation of ω_S (by SM-DTS) agrees with that of ω_D (by drying method) and both reflect the soil moisture content distribution from A to B. If ω_D is regarded as the precise value, the absolute errors (AE) of ω_S from 19 samples collected in every meter are shown in Table 2.

As shown in Table 2, the absolute errors of the 16 samples are all less than 3%, and the minimum is 0.01%. The other absolute errors are slightly higher, ranging from 2.97% to 6.57%. These relatively

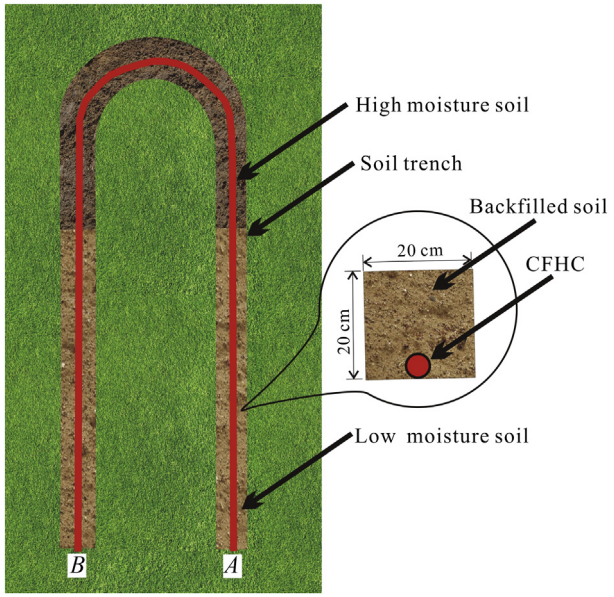

Fig. 10. Diagram of the soil trench with a 19 m length and a 20 cm × 20 cm cross-section in the field test.

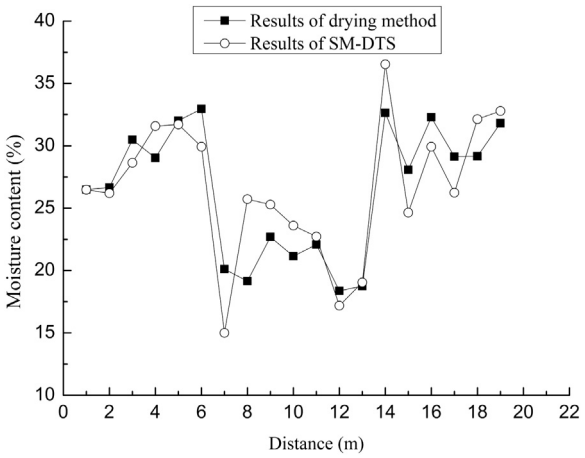

Fig. 11. Comparison of soil moisture content measured by drying method (ω_D) and SM-DTS (ω_S) in a 19 m long field test.

Table 2
Absolute errors between SM-DTS and drying method.

Distance from collection location to position *A* (m)	ω_D (%)	ω_S (%)	*AE* (%)
1	26.48	26.49	0.01
2	26.67	26.2	0.47
3	30.49	28.64	1.85
4	29.03	31.58	2.55
5	32.01	31.71	0.3
6	32.95	29.98	2.97
7	20.11	14.99	5.12
8	19.15	25.72	6.57
9	22.7	25.28	2.59
10	21.15	23.6	2.44
11	22.08	22.72	0.65
12	18.37	17.18	1.18
13	18.75	19.05	0.3
14	32.63	36.53	3.9
15	28.08	24.65	3.43
16	32.28	29.93	2.35
17	29.14	26.24	2.9
18	29.17	32.13	2.97
19	31.82	32.78	0.96

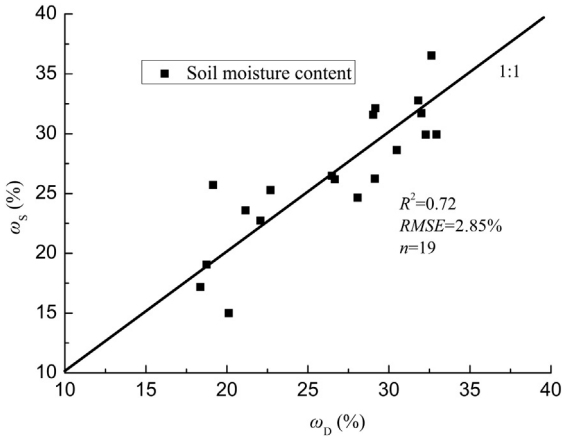

Fig. 12. Error analysis of the results measured by SM-DTS.

high errors may be caused by variations in soil composition and properties including root of plants, non-uniformity of dry densities, etc. Fig. 12 shows the error analysis of the results measured by SM-DTS as compared to ω_D.

As can be seen from Fig. 12, the data measured by the two methods have a relevance with $R^2 = 0.72$ and $RMSE = 2.85\%$. Comparing with the measurement accuracy of other methods proposed by other researchers (e.g. Calamita et al., 2012; Rowlandson et al., 2013; Yin et al., 2013), current study has higher relevance. The measuring result indicates that the SM-DTS has good measurement accuracy for the in-situ soil moisture content.

6. Conclusions

In conclusion, the following observations can be made about the SM-DTS method suggested in this paper:

(1) The CFHC is made with embedded sensing optical fiber and is shown to enhance measurement accuracy of soil moisture content. Temperature–time curves for soil moisture content correlations have been obtained in the laboratory.
(2) A temperature characteristic value (T_t) is proposed, and the relationship among T_t, soil thermal impedance and moisture content is established. Based on this relationship, the soil moisture content can be measured by the proposed DTS system.
(3) A distributed soil moisture measurement system (SM-DTS) is designed and made, which includes three subsystems: heating-sensing, demodulating and data processing.
(4) The parameters *k* and *b* of the SM-DTS are essential in soil moisture content measurement and can be determined in the laboratory.

The field results show that the SM-DTS method is viable for distributed measurements of in-situ soil moisture content, which has better results than previously proposed methods. For future studies, it is important to theoretically analyze the influences of intrinsic factors such as soil density and soil composition, and to establish relationship between temperature and soil moisture content by Richard's equation of soil moisture content and Fick's law.

Conflict of interest

We wish to confirm that there are no known conflicts of interest associated with this publication and there has been no significant financial support for this work that could have influenced its outcome.

Acknowledgments

The authors would like to thank all participants in the laboratory and field tests. The financial supports provided by the National Natural Science Foundation of China (Grant Nos. 41230636, 41372265, 41427801), and National Basic Research Program of China (973 Project) (Grant No. 2011CB710605) are gratefully acknowledged.

References

Abbasy F, Hassani FP, Madiseh SAG, Côté J, Nokken MR. An experimental study on the effective parameters of thermal conductivity of mine backfill. Heat Transfer Engineering 2014;35(13):1209–24.
Abu-Hamdeh N, Reeder RC. Soil thermal conductivity: effects of density, moisture, salt concentration, and organic matter. Soil Science Society of America Journal 2000;64(4):1285–90.
Barry-Macaulay D, Bouazza A, Singh RM, Wang B, Ranjith PG. Thermal conductivity of soils and rocks from the Melbourne (Australia) region. Engineering Geology 2013;164:131–8.

Benítez-Buelga J, Sayde C, Rodríguez-Sinobas L, Selker JS. Heated fiber optic distributed temperature sensing: a dual-probe heat-pulse approach. Vadose Zone Journal 2014;13(11). http://dx.doi.org/10.2136/vzj2014.02.0014.
Calamita G, Brocca L, Perrone A, Piscitelli S, Lapenna V, Melone F, Moramarco T. Electrical resistivity and TDR methods for soil moisture estimation in central Italy test-sites. Journal of Hydrology 2012;454–455:101–12.
Cho E, Choi M. Regional scale spatio-temporal variability of soil moisture and its relationship with meteorological factors over the Korean peninsula. Journal of Hydrology 2014;516:317–29.
Chung S, Horton R. Soil heat and water flow with a partial surface mulch. Water Resources Research 1987;23(12):2175–86.
Ciocca F, Lunati I, van de Giesen N, Parlange MB. Heated optical fiber for distributed soil-moisture measurements: a lysimeter experiment. Vadose Zone Journal 2012;11(4):1–10.
Côté A, Carrier B, Leduc J, Noël P, Beauchemin R, Soares M, Garneau C, Gervais R. Water leakage detection using optical fiber at the Peribonka dam. In: Proceedings of the 7th International Symposium on Field Measurements in Geomechanics. American Society of Civil Engineers; 2007. p. 1–12.
Côté J, Konrad JM. A generalized thermal conductivity model for soils and construction materials. Canadian Geotechnical Journal 2005;42(2):443–58.
Dobriyal P, Qureshi A, Badola R, Hussain SA. A review of the methods available for estimating soil moisture and its implications for water resource management. Journal of Hydrology 2012;458–459:110–7.
Doolittle JA, Collins ME. Use of soil information to determine application of ground penetrating radar. Journal of Applied Geophysics 1995;33(1–3):101–8.
Gil-Rodríguez M, Rodríguez-Sinobas L, Benítez-Buelga J, Sánchez-Calvo R. Application of active heat pulse method with fiber optic temperature sensing for estimation of wetting bulbs and water distribution in drip emitters. Agricultural Water Management 2012;120:72–8.
Grattan KTV, Sun T. Fiber optic sensor technology: an overview. Sensors Actuators A: Physical 2000;82(1–3):40–61.
Hartog AH. A distributed temperature sensor based on liquid core optical fibers. Journal of Lightwave Technology 1983;1(3):498–509.
Jougnot D, Revil A. Thermal conductivity of unsaturated clay-rocks. Hydrology and Earth System Sciences 2010;14(1):91–8.
Lu S, Ren T, Gong Y, Horton R. An improved model for predicting soil thermal conductivity from water content at room temperature. Soil Science Society of America Journal 2007;71(1):8–14.
Lunt IA, Hubbard SS, Rubin Y. Soil moisture content estimation using ground-penetrating radar reflection data. Journal of Hydrology 2005;307(1–4):254–69.
Luo GY, Li SL. Principles of engineering geology. Nanjing: Nanjing University Press; 1990.
Maleki M, Bayat M. Experimental evaluation of mechanical behavior of unsaturated silty sand under constant water content condition. Engineering Geology 2012;141–142:45–56.
Markle JM, Schincariol RA, Sass JH, Molson JW. Characterizing the two-dimensional thermal conductivity distribution in a sand and gravel aquifer. Soil Science Society of America Journal 2006;70(4):1281–94.
Mittelbach H, Lehner I, Seneviratne SI. Comparison of four soil moisture sensor types under field conditions in Switzerland. Journal of Hydrology 2012;430–431:39–49.
Read TO, Bour JS, Selker VF, Bense T, Borgne R, Hochreutener LN. Active-distributed temperature sensing to continuously quantify vertical flow in boreholes. Water Resources Research 2014;50(5):3706–13.
Rowlandson TL, Berg AA, Bullock PR, Ojo ER, McNairn H, Wiseman G, Cosh MH. Evaluation of several calibration procedures for a portable soil moisture sensor. Journal of Hydrology 2013;498:335–44.
Sayde C, Buelga JB, Rodriguez-Sinobas L, Khoury LE, Engish M, van de Giesen N, Selker JS. Mapping variability of soil water content and flux across 1–1000 m scales using the actively heated fiber optic method. Water Resources Research 2014;50(9):7302–17.
Sayde C, Gregory C, Gil-Rodriguez M, Tufillaro N, Tyler S, van de Giesen N, Selker JS. Feasibility of soil moisture monitoring with heated fiber optics. Water Resources Research 2010;46(6):1–8.
Schmugge TJ, Jackson TJ, McKim HL. Survey of methods for soil moisture determination. Water Resources Research 1980;16(6):961–79.
Schrott L, Sass O. Application of field geophysics in geomorphology: advances and limitations exemplified by case studies. Geomorphology 2008;93(1–2):55–73.
Steele-Dunne SC, Rutten MM, Krzeminska DM, Hausner M, Tyler SW, Selker J, Bogaard TA, van de Giesen N. Feasibility of soil moisture estimation using passive distributed temperature sensing. Water Resources Research 2010;46(3):1–12.
Striegl AM, Loheide SP. Heated distributed temperature sensing for field scale soil moisture monitoring. Ground Water 2012;50(3):340–7.
Sun YK, Li Q, Li XY, Yang DX. Progress of real-time monitoring technology in oil and gas industry based on fiber Bragg grating sensing. Science & Technology Review 2015;33(12). http://dx.doi.org/10.3981/j.issn.1000-7857.
Susha Lekshmi SU, Singh DN, Baghini MS. A critical review of soil moisture measurement. Measurement 2014;54:92–105.
Tyler SW, Selker JS, Hausner MB, Hatch CE, Torgersen T, Thodal CE, Geoffrey Schladow S. Environmental temperature sensing using Raman spectra DTS fiber-optic methods. Water Resources Research 2009;45(4):1–11.
Vogt T, Schneider P, Hahn-Woernle L, Cirpka OA. Estimation of seepage rates in a losing stream by means of fiber-optic high-resolution vertical temperature profiling. Journal of Hydrology 2010;380(1–2):154–64.
Weihermüller L, Huisman JA, Lambot S, Herbst M, Vereecken H. Mapping the spatial variation of soil water content at the field scale with different ground penetrating radar techniques. Journal of Hydrology 2007;340(3–4):205–16.
Weiss JD. Using fiber optics to detect moisture intrusion into a landfill cap consisting of a vegetative soil barrier. Journal of the Air & Waste Management Association 2003;53(9):1130–48.
Wierenga PJ, Nielsen DR, Hagan RM. Thermal properties of a soil based upon field and laboratory measurements. Soil Science Society of America Journal 1969;33(3):354–60.
Yin Z, Lei T, Yan Q, Chen Z, Dong Y. A near-infrared reflectance sensor for soil surface moisture measurement. Computers and Electronics in Agriculture 2013;99:101–7.

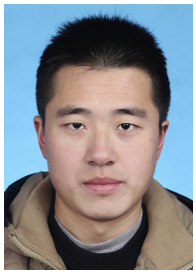

Dingfeng Cao is currently pursuing a Ph.D. degree in geological engineering from Nanjing University, China. He is mainly engaged in engineering geological research and the application of distributed fiber optic sensors in monitoring soil moisture. **Contact information**: School of Earth Sciences and Engineering, Nanjing University, 163 Xianlin Avenu, Nanjing, 210023, China. Tel.: +86-18205187501. E-mail: caodingfeng2014@gmail.com